

Stochastic Bifurcations in the Nonlinear Parallel Ising Model

Franco Bagnoli

*Dipartimento di Fisica e Astronomia and CSDC,
Università di Firenze, Via G. Sansone 1, I-50019 Sesto Fiorentino,
Italy, also INFN, sez. Firenze. email:franco.bagnoli@unifi.it*

Raúl Rechtman

*Instituto de Energías Renovables, Universidad Nacional Autónoma de México Apdo. Postal 34,
62580 Temixco, Mor., Mexico. email:rrs@ier.unam.mx*

We investigate the phase transitions of a nonlinear, parallel version of the Ising model, characterized by an antiferromagnetic linear coupling and ferromagnetic nonlinear one. This model arises in problems of opinion formation. The mean-field approximation shows chaotic oscillations, by changing the couplings or the connectivity. The spatial model shows bifurcations in the average magnetization, similar to what seen in the mean-field approximation, induced by the change of the topology, after rewiring short-range to long-range connection, as predicted by the small-world effect. These coherent periodic and chaotic oscillations of the magnetization reflect a certain degree of synchronization of the spins, induced by long-range couplings. Similar bifurcations may be induced in the randomly connected model by changing the couplings or the connectivity and also the dilution (degree of asynchronism) of the updating. We also examined the effects of inhomogeneity, mixing ferromagnetic and antiferromagnetic coupling, which induces an unexpected bifurcation diagram with a “bubbling” behavior, as also happens for dilution.

PACS numbers: 05.45.Ac,05.50.+q,64.60.aq,64.60.Ht

I. INTRODUCTION

There are quite a large number of studies about opinion formation in uniform societies [1–11]. Many such models adopt an approach similar to that of the Ising model. In such cases one has two opinions, say A and B or -1 and 1, and one is interested in the establishment of a majority (magnetic phase transitions) or in the effects of borders, or in the influence of some leader (social impact theory) [12]. This opinion space can be seen as the first ingredient of these models.

The second ingredient is how to model the response to an external influence. It is common to classify the attitude of people (agents) as either conformist or contrarian (also known as nonconformist). A conformist tends to agree with his neighbors and a contrarian to disagree.

It is also easy to map this attitude onto Ising terms: conformist agents correspond to ferromagnetic coupling and contrarians to antiferromagnetic ones [3]. The effects induced by the presence of contrarian agents in a society have been studied in models related to the voter model [13–25].

In general, agents that are under a strong social pressure tend to agree with the great majority even when they are certain that the majority’s opinion is wrong, as shown by Asch [26]. Under a strong social pressure a contrarian may agree with a large majority, an phenomenon that may be modelled using non-linear interactions.

The strategy of following an overwhelming majority may be ecological, since it is probable that this coherent behavior is due to some unknown piece of information, and in any case the competitive loss is minimal since it equally affects all other agents.

A binary opinion model where an agent tends to align with the largest neighboring cluster, similar to an Ising model with plaquette interactions, was studied in Ref. [27]. In this model, a single dissenting agent immersed in a cluster of different opinions cannot overcome the social pressure, and therefore the model exhibits absorbing homogeneous phases. The possibility of dissenting, distributed as a quenched disorder, was introduced in Ref [28].

The third ingredient is the connectivity, i.e., how the neighborhood of a given agent is composed. Traditionally, magnetic systems have been studied either on regular lattices, trees or with random connections, whose behavior is similar to that of the mean-field approach. In recent years, much attention has been devoted to other network topologies, like the small-world [29] to scale-free [30] etc.

The Ising model has been studied in different topologies [31–34], in particular, the topological details may affect the critical dynamics [35] and the zero-temperature quench [36].

In contrast with the Ising model, in the study of opinion formation there is no compulsory obligation to have symmetric interactions, each agent is influenced by those in his neighborhood, which are not necessarily influenced by the first agent.

Each individual may be a conformist or a contrarian and this character does not change in time. In these terms, the simple ferromagnetic Ising model represents a uniform society of conformists with local symmetric interactions.

The fourth ingredient is the update scheduling, that may be completely asynchronous, like in standard Monte

Carlo simulations, or completely parallel, like in Cellular Automata, or something in between [38–40]. It is not clear which scheme is the most representative of reality. Real human interactions are indeed continuous, but also clocked by days, elections, etc.

An effect that is favoured by parallelism is synchronization in the presence of complex dynamics. As happens in physics, a macroscopic irregular behavior (macroscopic chaos) implies a coherent, although irregular motion of many elements (the microscopic constituents).

One of most intriguing effects is the hipster’s one, in which a society of contrarians tends to behave in a uniform way [37]. Clearly, “conformist hipsters” always change their behavior, when they realize to be still in the mainstream, but since they do so all together, they remain synchronized: the parallelism is a crucial element of such a behavior.

Finally, the fifth ingredient is homogeneity. There are many possibilities of introducing mixtures of agents or spins with different coupling. We investigate what happens when one mixes ferromagnetic and antiferromagnetic interactions, and we shall show that this mixture promotes a “bubbling” behavior in the bifurcation, meaning that the bifurcation appears first for intermediate values of the parameters, similar to what happens with asynchronism.

In previous studies we presented “reasonable contrarian” agents whose response to the average opinion of their neighbors is nonlinear and discussed the collective behavior of societies composed of reasonable contrarians only and by mixtures of these agents and nonlinear conformists [24, 25]. The rationale was that in some cases, and in particular in the presence of frustrated situations like in minority games [41–44], it is not convenient to always follow the majority, since in this case one is always on the “losing side” of the market. This is one of the main reasons for the emergence of a contrarian attitude. On the other hand, if all or almost all agents in a market take the same decision, it is often wise to follow such a trend. We can denote such a situation with the word “social norm”.

A society composed by a strong majority of reasonable contrarians exhibits interesting behaviors when changing the topology of the connections. On a one-dimensional regular lattice, there is no long-range order, the evolution is disordered and the average opinion is always halfway between the extreme values [45]. However, adding long-range connections or rewiring existing ones, we observe the Watts-Strogatz “small-world” effect, with a transition towards a mean-field behavior. But since in this case the mean-field equation is, for a suitable choice of parameters, chaotic, we observe the emergence of coherent oscillations, with a bifurcation cascade eventually leading to a chaotic-like behavior of the average opinion.

The small-world transition is essentially a synchronization effect. Similar effects with a bifurcation diagram resembling that of the logistic map have been observed in a different model of “adapt if novel - drop if ubiquitous”

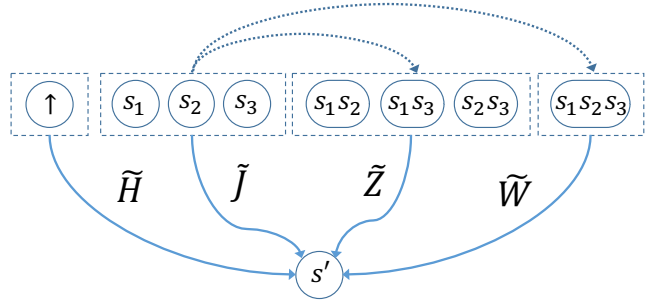


FIG. 1. (Color online.) A $K = 3$ spin neighborhood, with the interaction terms corresponding to the external field \tilde{H} , the two-spin \tilde{J} , three-spin \tilde{Z} , and four-spin \tilde{W} interaction constants.

behavior, upon changing the connectivity [46, 47].

The main goal of the present study is that of reformulating the opinion formation models mentioned above [24, 25], in terms of a parallel, nonlinear Ising model both on a regular lattice, where the spin at any site is influenced by its nearest neighbors, and on small-world networks.

In the first case the mean-field behavior of the magnetization is described by a nonlinear equation for which chaos can be evaluated by the Lyapunov exponent [53], which is a measure of the stability of trajectories.

The Lyapunov exponent is the time average of the growth rate of an initial infinitesimal perturbation of a trajectory. Clearly, this quantity cannot be simply defined for stochastic systems, since in this case one would essentially measure the effects of the noise. However, in many cases and in particular the present one, we would like to compare the dynamical properties of a stochastic microscopic model and its mean-field approximation. We show here that the Boltzmann’s entropy of an aggregate variable like the magnetization is a quantity that can be defined for both deterministic and stochastic systems. In the first case, Boltzmann’s entropy can be used as a measure of chaos [48].

The scheme of the paper is the following. We discuss the “nonlinear” parallel Ising model in Section II. We can therefore introduce the mean-field approximation of the model in Section III, showing the bifurcation phase diagrams as a function of the parameters. The definition of the entropy and the results of microscopic simulations η are reported in Section IV. Finally, conclusions are drawn in the last Section. In this Section we discuss also the differences between the present and the original model of Refs. [24, 25].

II. PARALLEL NONLINEAR ISING MODEL

We consider a system with N sites, each one in a state $s_i \in \{-1, 1\}$, $i = 1, \dots, N$. The state of the system is $\mathbf{s} =$

(s_1, \dots, s_N) . The topology of the system is defined by the adjacency matrix a with $a_{ij} = 1$ if site j belongs to site i 's neighborhood and is zero otherwise. The connectivity k_i , the local field \tilde{h}_i , and the rescaled local field h_i at site i are

$$k_i = \sum_j a_{ij}, \quad \tilde{h}_i = \sum_j a_{ij}s_j, \quad h_i = \frac{\tilde{h}_i}{k_i},$$

with $h_i \in [-1, 1]$. In this paper we shall use a uniform connectivity $k_i = K \forall i$. The magnetization m is defined as

$$m = \frac{1}{N} \sum_i s_i,$$

with $m \in [-1, 1]$.

In the following we consider multi-spin (plaquette) interactions. We moreover consider only completely asymmetric interactions [49, 50], arranged to give a preferred direction that corresponds to time in the standard cellular automata language [24, 51].

Considering up to 4-spin interactions, the Hamiltonian is

$$\mathcal{H}(\mathbf{s}) = - \sum_i s'_i \left(\tilde{H} + \tilde{J} \sum_j a_{ij}s_j + \tilde{Z} \sum_{jk} a_{ij}a_{ik}s_js_k + \tilde{W} \sum_{jkl} a_{ij}a_{ik}a_{il}s_js_ksl \right), \quad (1)$$

where \tilde{H} is the external field, and \tilde{J} , \tilde{Z} , \tilde{W} the two-spin, three-spin and four-spin interaction constants respectively as shown in Fig. 1.

It is possible to recast the interaction constants in terms of the local field h_i . The terms containing s'_i at "time" $t + 1$ are,

$$\begin{aligned} \text{2-spin: } & s'_i \sum_j a_{ij}s_j = s'_i \tilde{h}_i, \\ \text{3-spin: } & s'_i \sum_{jk} a_{ij}a_{jk}s_js_k = s'_i Q_i^{(2)}, \\ \text{4-spin: } & s'_i \sum_{jkl} a_{ij}a_{ik}a_{il}s_js_ksl = s'_i Q_i^{(3)}. \end{aligned}$$

These expressions define $Q^{(2)}$ and $Q^{(3)}$. Since

$$\begin{aligned} \tilde{h}_i^2 &= K + 2Q_i^{(2)}, \\ \tilde{h}_i^3 &= (3K - 2)\tilde{h}_i + 6Q_i^{(3)}, \end{aligned}$$

the Hamiltonian can be written as

$$\mathcal{H}(\mathbf{s}) = - \sum_i s'_i (H + Jh_i + Zh_i^2 + Wh_i^3), \quad (2)$$

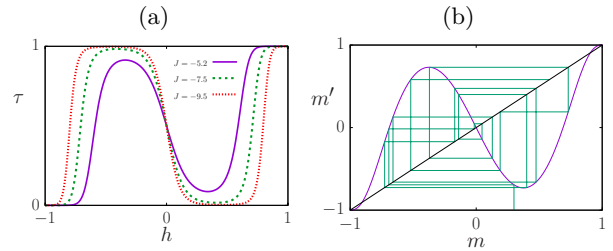


FIG. 2. (Color online). (a) The transition probability $\tau = \tau(1|h)$, Eq. (3) as a function of the local field h for three values of the coupling constant J . (b) Graph of the magnetization m' at time $t + 1$ as a function of the magnetization m at time t , Eq. (4), with some iterates for $J = -7.5$.

where the correspondences among coupling constants are

$$\begin{aligned} H &= \tilde{H} - \frac{1}{2}K\tilde{Z}, \\ J &= K \left(\tilde{J} - \frac{3K - 2}{6}\tilde{W} \right), \\ Z &= \frac{1}{2}K^2\tilde{Z}, \\ W &= \frac{1}{6}K^3\tilde{W}. \end{aligned}$$

In the following, we shall consider pair (J) and four-spin (W) terms, *i.e.*, $H = Z = 0$, in agreement with previous investigations [24].

The coupling term J modulates the "linear" effects of neighbors, so $J > 0$ gives a conformist (ferromagnetic) behavior and $J < 0$ a contrarian (antiferromagnetic) one. The term W modulates the nonlinear effects of the crowd. In this way one can model the Asch effect by inserting $J < 0$ (contrarian attitude) and $W > 0$ (social norms).

The time evolution of the spins is given by the parallel application of the transition probabilities $\tau(s'_i|h_i)$ that gives the probability that the spin at site i and time $t + 1$ takes value s'_i given the local field h_i at time t , see Fig. 1. The local transition probability is defined by a heat bath probability

$$\begin{aligned} \tau(s'_i|h_i) &= \frac{1}{1 + \exp(-2s'_i(Jh_i + Wh_i^3))} \\ &= \frac{1}{2} [1 + s'_i \tanh(Jh_i + Wh_i^3)]. \end{aligned} \quad (3)$$

The parallel version of the linear ($W = 0$) Ising model does not show many differences with respect to the standard serial one [38]. The observables that depend only on single-site properties take the same values in parallel or sequential dynamics [39], although differences arise for two-site correlations [52]. In general the resulting dynamics is no more reversible with respect to the Gibbs measure induced by any Hamiltonian [40].

In the following, unless otherwise specified, we always use $W = 15$ and $K = 20$.

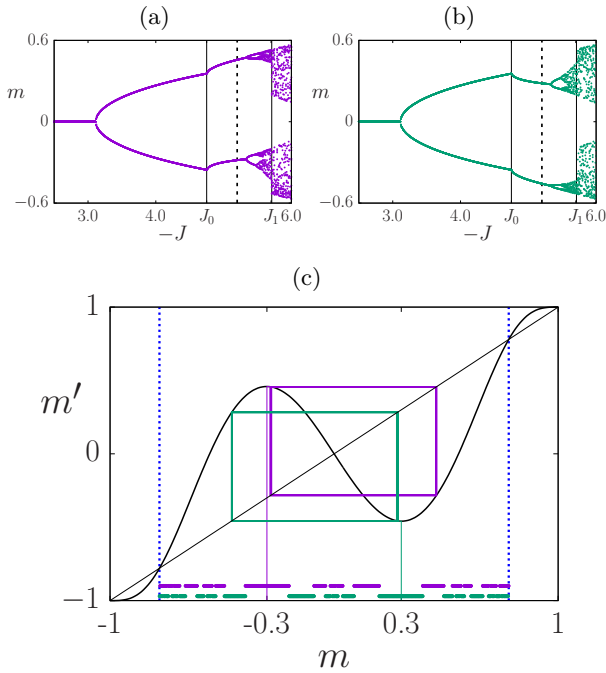


FIG. 3. (Color online). (a) Mean-field bifurcation diagrams of the magnetization m for initial magnetization $m_0 = -0.3$ in (a) and $m_0 = 0.3$ in (b), as functions of the linear coupling J . In (a) and (b), the vertical dotted lines (in black) are drawn at $J = -5.2$ and the vertical continuous lines (in black) at $J_0 = -4.75$ and $J_1 = -5.71$. Between these values, the bifurcation diagram depends on the initial magnetization m_0 . In (c) the return map of Eq (4) for $J = -5.2$ corresponding to the dotted line in the previous figures. The vertical lines mark the basins of attraction of the two period-2 orbits. The dots in the bottom part (in green) mark the basin including $m_0 = 0.3$ corresponding to the leftmost orbit (also in green) and figure (b), while the dots above them (in magenta) mark the basin including $m_0 = -0.3$, corresponding to the rightmost orbit (also in magenta) and figure (a).

III. MEAN-FIELD APPROXIMATION

The mean-field approximation for the magnetization m of the fully parallel case with fixed connectivity K , follows from the Markov equation assuming no spatial correlations. Then

$$m' = f(m) = \frac{1}{2^K} \sum_{k=0}^K \binom{K}{k} (1+m)^k (1-m)^{K-k} \times \tanh \left[J \left(\frac{2k}{K} - 1 \right) + W \left(\frac{2k}{K} - 1 \right)^3 \right], \quad (4)$$

with $m = m(t)$ and $m' = m(t+1)$. We show in Fig. 2 (b) the graph of m' together with some iterates of the map.

The mean-field magnetization exhibits chaos that can be characterized by the Lyapunov exponent λ [53]. However, on spatially extended networks m changes stochastically and cannot be characterized in the same way.

In order to compare microscopic and mean-field models within the same framework we use the Boltzmann's entropy η [24, 48] of the magnetization m . The interval $[-1, 1]$ is partitioned in L disjoint intervals I_i of equal size and the probability q_i of I_i is the fraction of visits to I_i after T time steps with $T \gg 1$.

Once these probabilities are known, η is defined by

$$\eta = -\frac{1}{\log L} \sum_{i=1}^L q_i \log q_i, \quad (5)$$

so that $0 \leq \eta \leq 1$, the lower bound corresponding to a fixed point, the upper one to the uniform distribution $q_i = 1/L$.

For a periodic orbit of period 2^p and $L = 2^b$, $\eta = p/b$. For low-dimensional dynamical systems, like the mean-field equation, the mid-value threshold $\eta = 0.5$ effectively separates the contracting dynamics (cycles) from the chaotic ones. For spatially-extended systems, there is always a stochastic noise that increases the value of the entropy in the “fixed-point” part of the parameter space. This base-level value is related to the size of the sample, and slowly vanishes for large samples.

In order to use finite-size samples, we set the onset of the phase in the stochastic systems corresponding to the chaotic phase in the deterministic ones to the mid-value of the range of η . Taking the limits $T \rightarrow \infty$, $L \rightarrow \infty$ leads to the Kolmogorov-Sinai entropy [53–56].

Before presenting the different scenarios, let us illustrate the type of bifurcations that are present. In Figs. 3 (a) and (b) we show parts of the bifurcation diagram of the map of Eq. (4) as a function of J starting with different values of the initial magnetization m_0 .

Referring to the values in the Figure, at $J = J_0$ there is a pitchfork bifurcation, i.e., a separation of basins, that reunite at $J = J_1$, which is another pitchfork bifurcation, in the reverse direction. Intermixed, there are period-doubling bifurcations. There are other pitchfork bifurcations for different intervals of J .

In Fig. 3 (c) we show the return map of the mean-field map for $J = -5.2$. We can see that there are four basins of attraction. For small values of the initial magnetization m_0 , the orbit is attracted to $m = -1$ and for large m_0 to $m = 1$. The regions where this occurs are marked by the vertical dotted lines in the Figure. For other values of m_0 , m ends in one of two period-two orbits. This figure shows, in the lower part, the two basins of attraction that are symmetric in the sense that if m_0 belongs to one basin of attraction, $-m_0$ belongs to the other one.

In what follows we present the bifurcation diagrams of the mean-field map Eq. (4) by varying the coupling constants J and W . Unless otherwise noticed, we computed the Lyapunov exponent λ by averaging over 10,000 time steps after a transient of another 10,000 steps. The entropy η was computed using 256 boxes and 25,000 time steps.

In Fig. 4 (a) we show the bifurcation diagram of the magnetization m , Eq. (4), as a function of J with W and

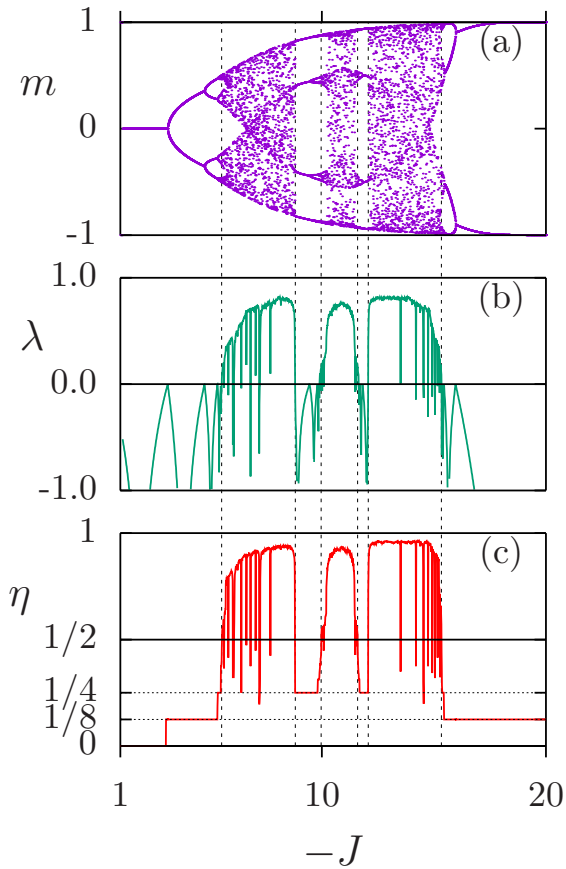


FIG. 4. (Color online.) (a) Bifurcation diagram of the mean-field map of the magnetization m , Eq. (4), as a function of the linear coupling J . In (b) the corresponding Lyapunov exponent λ and in (c) the entropy η . The vertical dotted lines are drawn at the estimated values of J for which $\lambda = 0$. The horizontal dotted lines in (c) correspond to period 2, $\eta = 1/8$, and period 4, $\eta = 1/4$, orbits. For every value of J , two initial values of the magnetization were used, $m_0 = -0.3$ and $m_0 = 0.3$.

K fixed. The diagram exhibits a period doubling cascade towards chaos with periodic windows and pitchfork bifurcations.

The bifurcation diagram of m as a function of W with J and K fixed is shown in Fig. 5 (a). In this case, there is an inverse period doubling cascade to chaos with pitchfork bifurcations.

The next row of figures, Figs. 4 (b) and Fig. 5 (b), show the corresponding Lyapunov exponent λ , and the last one, Figs. 4 (c) and Fig. 5 (c), the entropy η . The dotted vertical lines are drawn at some of the values of J or W where λ passes from a negative to a positive value or vice versa. These values coincide to jumps of η from values smaller to $1/2$ to larger ones or vice versa and mark the appearance of chaos or periodic windows in the bifurcation diagrams.

Therefore, η can be used as a measure of chaos. To stress this, we show in Figs. 6 the mean-field phase di-

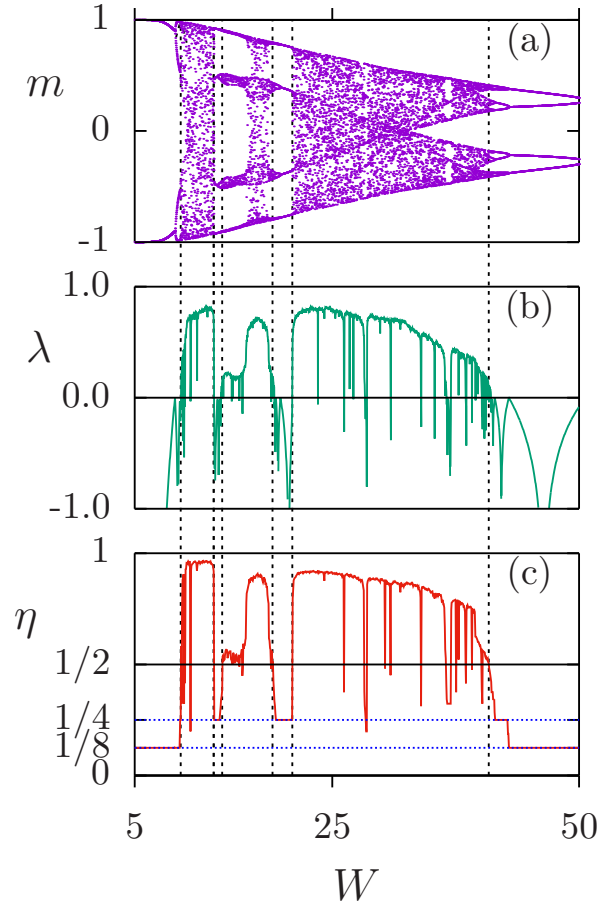


FIG. 5. (Color online.) (a) Bifurcation diagram of the mean-field map of the magnetization m , Eq. (4), as a function of the coupling constant W with $J = -10$. In (b) The corresponding Lyapunov exponent λ and in (c) the entropy η . The vertical dotted lines are drawn at the estimated values of W for which $\lambda = 0$. The horizontal dotted lines in (c) correspond to period 2, $\eta = 1/8$, and period 4, $\eta = 1/4$, orbits. For every value of W , two initial values of the magnetization were used, $m_0 = -0.3$ and $m_0 = 0.3$.

agrams of λ (top) and η (bottom). These diagrams are similar. The horizontal lines at $W = 15$ correspond to Figs. 4 (b) and (c) and the vertical ones at $J = -10$ to Figs. 5 (b) and (c) respectively. We find a similar behavior of the mean-field map as K varies with fixed J and W . The three quantities J , W and K are related by scaling relations, as shown in the Appendix.

The dotted horizontal lines in Fig. 4 (c) and Fig. 5 (c) correspond to period 2, $\eta = 1/8$, and period 4, $\eta = 1/4$ orbits. Looking at the bifurcation diagram in Fig. 4 (a), for small $-J$, the map has a fixed point and as $-J$ grows there is a first bifurcation to a period 2 orbit and another one to what looks like a period 4 orbit, but $\eta = 1/8$ instead of $\eta = 1/4$ for period 4 orbits. What appears like a bifurcation to period four orbits is actually a pitchfork bifurcation to two period-two orbits that depend on the initial magnetization m_0 as mentioned before. There are

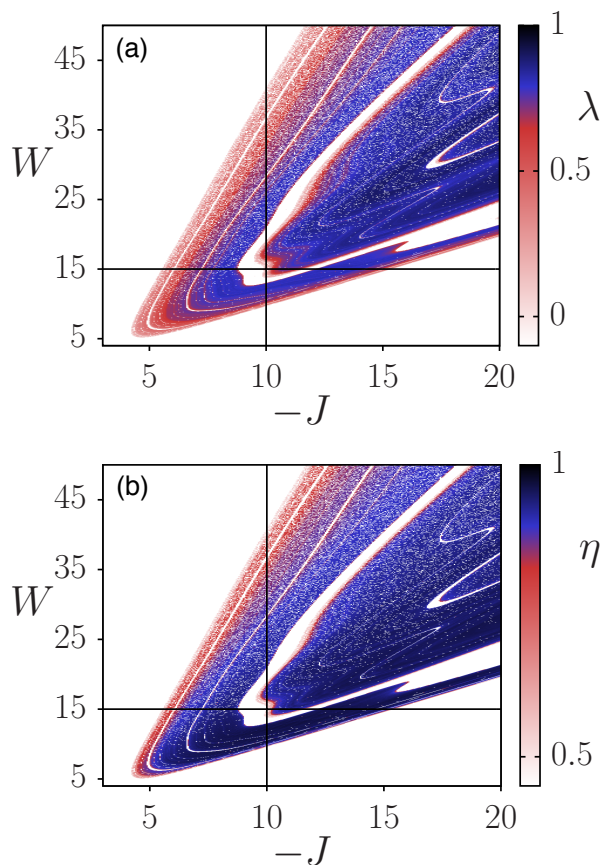


FIG. 6. (Color online) (a) Mean-field phase diagram of the Lyapunov exponent λ showing the values of $(-J, W)$ where $\lambda > 0$. (b) The mean-field phase diagram of the entropy showing the values of $(-J, W)$ where $\eta > 1/2$.

other pitchfork bifurcations for other values of J with W fixed and also for values of W with J fixed.

IV. SMALL-WORLD STOCHASTIC BIFURCATIONS

In the Watts-Strogatz small-world model [29], starting with a network where every site has K nearest neighbors, at any site i , with probability p , known as the long-range connection probability, each one of its K neighbors is replaced by a random one. Then the spin at each site is updated according to Eq. (3). As p grows, coherent oscillations of a majority of spins begin to appear so that the magnetization m shows noisy periodic or irregular oscillations. The noise is the manifestation of the stochasticity of the updating rule. Similar patterns can be seen in Ref. [45], where the effect of the size of neighborhood is studied.

As shown in the following, by changing several parameters, we can obtain stochastic bifurcation diagrams similar to the mean-field ones. The following microscopic simulations were carried using lattices of $N = 10,000$

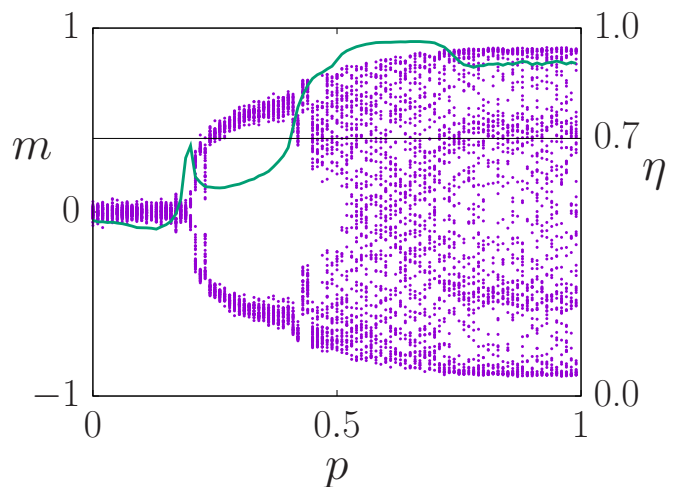


FIG. 7. (Color online) Small-world stochastic bifurcation diagram of the magnetization m , dots (in magenta), and the entropy η , continuous curve (in green), as functions of the long-range connection probability p with $J = -10$. The “jump” of m for $p \simeq 0.45$ corresponds to a pitchfork bifurcation (dependence on the initial magnetization).

sites, with a transient of 10,000 time steps. The entropy η was computed with 256 boxes and 25,600 time steps.

In Fig. 7 we show the bifurcation map and the entropy η as functions of p . There is always some disorder, even for small values of p where $m \sim 0$, and as p grows we find bifurcations and more disorder. Indeed, the entropy η is a good measure of this behavior, small values of η corresponding to noisy “periodic orbits” while larger ones to disorder (“chaos”).

In the mean-field case, we found $\eta = 1/2$ to be a good threshold to separate order from chaos. For the stochastic dynamics on small-world networks we choose as the threshold the approximate value of the entropy at the first bifurcation as shown in the figures. For values smaller than this threshold there are noisy periodic orbits. The bifurcation diagram of the figure is reminiscent of the mean-field one, Fig. 4.

Notice that pitchfork bifurcations (dependence on the initial magnetization) are present also in the microscopic simulations, as shown in Fig. 7

In Fig. 8 we show the bifurcation diagrams and entropy of the magnetization m for the small-world networks obtained for different values of p . As before, the entropy is a good indicator of disorder.

Clearly, by setting the rewiring probability p large enough, one can also recover the mean-field bifurcation diagrams as function of J , K and W , with a good correspondence of the critical values of parameters.

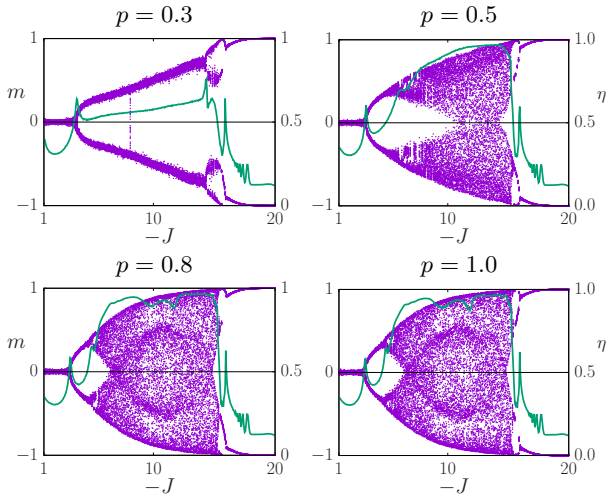


FIG. 8. (Color online) Small-world bifurcation diagram of the magnetization m , dots (in magenta) and the corresponding entropy η , continuous line (in green), as functions of the linear coupling constant J and different values of the long-range connection probability p .

A. Partial asynchronism (dilution)

The dilution d is the fraction of sites chosen at random that are not updated at every time step. We define the diluted rule as

$$s_i(t+1) = \begin{cases} 1 & \text{with probability } (1-d)\tau(1|h_i), \\ -1 & \text{with probability } (1-d)[1-\tau(1|h_i)], \\ s_i(t) & \text{otherwise, i.e., with probability } d, \end{cases} \quad (6)$$

so that for $d = 0$ one has the standard parallel updating rule. One time step is defined when on the average every site of the lattice is updated once. For a system with N sites, the smallest value of the dilution is $d = 1/N$ and then $t_d = 1/d$ updates are needed to complete one time step. If $d = 1/2$, $t_d = 2$, etc.

The mean-field equation corresponding to dilution is

$$m(t+1) = (1-d)m(t) + df(m(t));$$

where f is the the map of Eq. (4). The mean-field phase diagram is reported in Fig. 9. Notice that the border at $d = 0$ corresponds to the horizontal line in Fig. 6.

The bifurcation diagrams and the entropy η of the magnetization as functions of of the dilution d are shown in Fig. 10 for different value of the long-range connection probability p . It is interesting to note the “bubbling” transition: the oscillations are favored, for intermediate values of the rewiring p , by a non-complete parallelism.

As shown in the figure, for values of p larger than 0.1, the dilution is able to trigger bifurcations also in the spatial model. In contrast with the linear Ising model [40], where even a small amount of asynchronism is able to destroy the “effective” antiferromagnetic coupling, here the

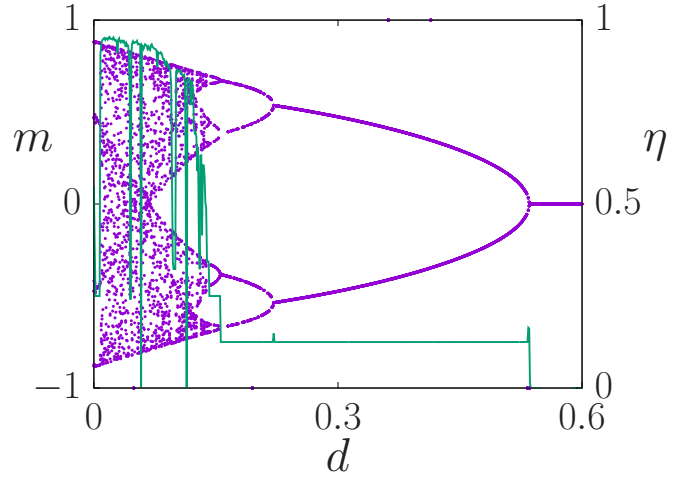


FIG. 9. (Color online) Mean-field bifurcation diagram of the magnetization m (dots in magenta, two initial conditions), and the entropy η (continuous curve in green), as functions of the dilution probability d with $J = -10$.

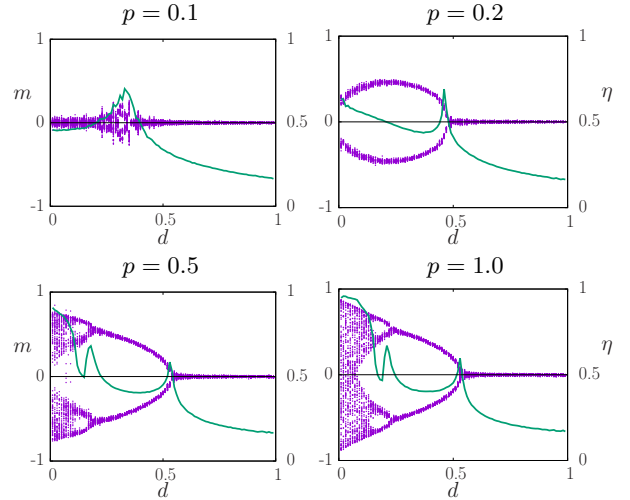


FIG. 10. (Color online). Bifurcation diagrams of the magnetization m on small-world networks, dots (in magenta), and the entropy η , continuous curve (in green), as functions of the dilution d with $J = -10$, and different values of the long-range connection probability p .

behavior is smooth with respect to dilution. See Ref. [52] for a study about metastable effects in the linear model.

B. Heterogeneity

In order to measure the effects of heterogeneity, we let a fraction ξ of spins interact ferromagnetically ($J > 0$) with their K neighbors and a fraction $1 - \xi$ interact antiferromagnetically ($J < 0$). We show in Fig. 11 the bifurcation diagrams of the magnetization m together with the en-

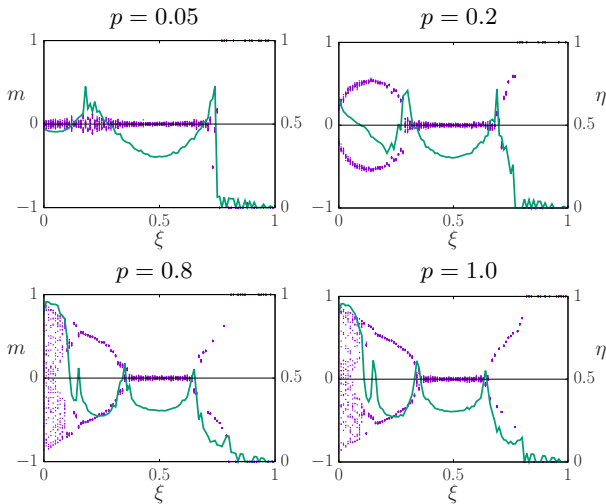


FIG. 11. (Color online.) Small-world ferro-anti ferro bifurcation diagram (left axis, dots in magenta) and entropy η (right axis, continuous curve in green) of the magnetization m as a function of ξ for different values of the long range probability p and $N = 10,000$, $|J| = 10$,. for $P = 0.05$ there is no threshold for η , for $p = 0.2$ it is $\eta = 0.7$, for $p = 0.8$ and $p = 1.0$ it is $\eta = 0.6$.

entropy η as functions of ξ for different values of p . Again, the entropy is a good measure of disorder. One can see a “bubbling” effect very similar to what observed by changing the dilution. In other words, oscillations, which are a product of antiferromagnetism and parallelism, are actually favoured by a small percentage of asynchronism and/or of ferromagnetic nodes, for a partial long-range rewiring of links.

V. CONCLUSIONS

We investigated the phase transitions of a nonlinear, parallel version of the Ising model, characterized by a linear coupling $J < 0$ and a nonlinear one $W > 0$. The mean-field approximation shows chaotic oscillations, by changing the couplings J and W or the connectivity K . We showed in the Appendix that there is a scaling relation among these parameters.

The nonlinear Ising model was studied on small-world networks, where p is the probability of long-range rewiring of links. Here, entropy of the magnetization becomes a measure of disorder which is adequate once a threshold between the presence and absence of noisy periodic orbits is established. The noisy periodic and disordered behavior of m imply a certain degree of synchronization of the spins, induced by long-range couplings.

We have shown also that similar bifurcations may be induced in the randomly connected model by changing the parameters J , the dilution factor d and the heterogeneity ξ , by mixing ferromagnetic and antiferromagnetic interactions.

In particular, we observed that a small percentage of asynchronism or of ferromagnetic nodes favours the first period-doubling bifurcation, which appears first for intermediate values of d and ξ .

This model is a generalization of an opinion formation model presented in Refs. [24] and [25]. In contrast with those investigations, we developed here the whole model within the framework of the parallel Ising model, with transition probabilities that are continuous and smooth, derived from Hamiltonian couplings. We found the mean-field bifurcation and phase diagrams as functions of J and W , and discussed the dynamics on small-world networks as functions of the long-range rewiring probability p and the heterogeneity ξ . The results are qualitatively similar to those found before, showing a certain degree of universality regardless of the details of the model.

We obtained also new results, such as the mapping among the parameters (only possible within this continuous approach) and the stochastic bifurcation phase diagram as function of the asynchronism (or dilution) d of the updating rule.

The different diagrams show a striking similarity, implying that it should be possible to map one bifurcation onto the other, as we did with the mean-field approach among J , W and K .

The present model aims at incorporating the Asch effect [26] in mean-field and microscopic simulations, *i.e.*, the influence of social pressure and its dominance over the “linear” contrarian predisposition. The resulting mean-field approach exhibits a chaotic behavior, which is our knowledge was rarely (if ever) observed before.

What is remarkable is the appearance of coherent oscillations of the whole population also for the microscopic model, in the presence of long-range connections (small-world). This may have important consequences for social scientists: the conflict between a liberal education (contrarian attitude) and the ever present social pressure may lead to unpredictable oscillation triggered by many quantities, in our widely connected world.

VI. APPENDIX

A. Continuous approximation and parameter mapping

The similarities among bifurcation diagrams with different connectivity K and coupling parameters J , W can be explained by using a continuous approximation of the mean-field equation.

By using Stirling’s approximation for the binomial co-

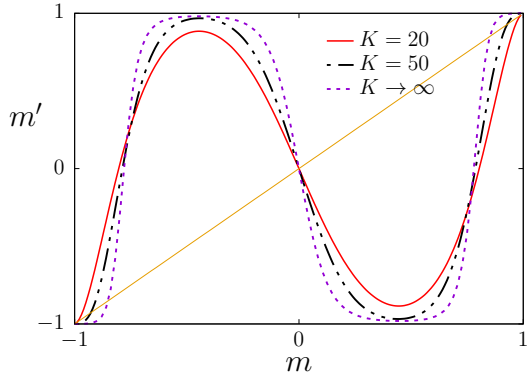


FIG. 12. (Color online.) Scaling relation Eq. (10) for three values of the connectivity K , with $J(K=20) = -10$ and $W(K=20) = 15m$, and the other values of J and W obtained from Eq. (10).

efficients in Eq. (4), for small values of m [53], we obtain

$$\frac{1}{2K} \binom{K}{k} (1+m)^k (1-m)^{K-k} \simeq \sqrt{\frac{2K}{\pi(1-m^2)}} \exp\left[-\frac{2K}{1-m^2} \left(\frac{k}{K} - \frac{1+m}{2}\right)^2\right] \quad (7)$$

and therefore, substituting $2k/K - 1 = x$,

$$m' = \sqrt{\frac{K}{2\pi(1-m^2)}} \times \int_{-\infty}^{\infty} dx \exp\left(-\frac{K(x-m)^2}{2(1-m^2)}\right) \tanh(Jx + Wx^3), \quad (8)$$

from which the convolution structure is evident.

By developing $\tanh(-Jx + Wx^3)$ at first order (i.e., large K and small values of m), we can compute the

convolution, obtaining after remapping the first terms in powers of m ,

$$m' = \tanh(\tilde{J}m + \tilde{W}m^3) \quad (9)$$

with

$$\begin{aligned} \tilde{J} &= J + \frac{3W}{K}, \\ \tilde{W} &= W \left(1 - \frac{3}{K}\right). \end{aligned} \quad (10)$$

Notice that in the limit $K \rightarrow \infty$, $\tilde{J} \rightarrow J$ and $\tilde{W} \rightarrow W$.

The relation between parameters J, K and J_1, K_1 of two mean-field approximations with different connectivities K and K_1 is

$$\begin{aligned} J_1 &= J + \frac{3}{K} W \left(1 - \frac{K-3}{K_1-3}\right), \\ W_1 &= W \frac{K_1}{K} \frac{K-3}{K_1-3}. \end{aligned} \quad (11)$$

Since the approximation of the hyperbolic tangent is valid for small x , we expect that this scaling is better for large K , for which the convolution length is small. In Fig. 12 we report the scaling correspondence for some values of K .

Since $J < 0$ and $K > 0$, the effect of this scaling is that of lowering the absolute value of \tilde{J} and \tilde{K} for small K (larger than 3), so, given that for a large value of K and certain values of J and W the mean-field equation is chaotic, it may be reduced to a fixed point graph by lowering the connectivity K .

ACKNOWLEDGMENTS

This work was partially supported by project PAPIIT-DGAPA-UNAM IN109213. F.B. acknowledges partial financial support from European Commission (FP7-ICT-2013-10) Proposal No. 611299 SciCafe 2.0.

-
- [1] R. Hegselmann, U. Krause, *Opinion dynamics and bounded confidence models, analysis, and simulation*, Journal of Artificial Societies and Social Simulation (JASSS) **5**, 1–33 (2002).
 - [2] G. Deffuant, D. Neau, F. Amblard, and G. Weisbuch, *Mixing beliefs among interacting agents*, Adv. Complex Syst. **3** 87 (2000). doi:10.1142/S0219525900000078
 - [3] C. Castellano, S. Fortunato and V. Loreto, *Statistical physics of social dynamics*, Rev. Mod. Phys. **81**, 591 (2009).
 - [4] D. Stauffer, *Sociophysics simulations II: opinion dynamics*, in *Modelling Cooperative Behavior in the Social Sciences*, AIP Conf. Proc. **779**, 56 (2005). doi:10.1063/1.2008591
 - [5] S. Galam, *Sociophysics: A review of Galam models*, International Journal of Modern Physics C **19**, 409 (2008). doi:10.1142/S0129183108012297
 - [6] S. Galam, *Sociophysics: A Physicist's Modeling of Psycho-Political Phenomena*, (Springer, 2012). doi:10.1007/978-1-4614-2032-3
 - [7] F. Bagnoli, T. Carletti, D. Fanelli, A. Guarino, A. Guazzini, *Dynamical affinity in opinion dynamics modeling*, Phys. Rev. E **76**, 066105 (2007). doi:10.1103/PhysRevE.76.066105
 - [8] F. Bagnoli, A. Guazzini, P. Liò, *Human heuristics for autonomous agents*, Bio-Inspired Computing and Communication LNCS 5151 (Springer 2008) p. 340. doi:10.1007/978-3-540-92191-2_30

- [9] R. Lauro Grotto, A. Guazzini, F. Bagnoli, *Metastable structures and size effects in small group dynamics*, *Frontiers in psychology* **5**, 699 (2014). doi:10.3389/fpsyg.2014.00699
- [10] A. Guazzini, A. Cini, F. Bagnoli, J.J. Ramasco, *Opinion dynamics within a virtual small group: the stubbornness effect*, *Frontiers in physics* **3**, 65 (2015). doi:10.3389/fphy.2015.00065
- [11] D. Vilone, T. Carletti, F. Bagnoli, A. Guazzini, *The Peace Mediator effect: Heterogeneous agents can foster consensus in continuous opinion models*, *J. Phys. A* **462**, 84 (2016). doi:10.1016/j.physa.2016.06.082
- [12] M. Lewenstein, A. Nowak, B. Latane, *Statistical mechanics of social impact* *Phys. Rev. A* **45**, 763 (1992). doi:10.1103/PhysRevA.45.763
- [13] N. Masuda, *Voter models with contrarian agents*, *Phys. Rev. E* **88** 052803 (2013). doi:10.1103/PhysRevE.88.052803
- [14] N. Crokidakis, V. H. Blanco, and C. Anteneodo, *Impact of contrarians and intransigents in a kinetic model of opinion dynamics*, *Phys. Rev. E* **89** 013310 (2014). doi:10.1103/PhysRevE.89.013310
- [15] P. Nyczka, K. Sznajd-Weron *Anticonformity or Independence?—Insights from Statistical Physics*, *J. Stat. Phys.* **151**, 174–202 (2013). doi:10.1007/s10955-013-0701-4
- [16] J.J. Schneider, *The influence of contrarians and opportunists on the stability of a democracy in the Sznajd model*, *Int. J. Mod. Phys. C*, **15** 659 (2004). doi:10.1142/S012918310400611X
- [17] M. S. de la Loma, J. M. López, and H. S. Wio, *Spontaneous emergence of contrarian-like behaviour in an opinion spreading model*, *Europhys. Lett.* **72** 851 (2005). doi:10.1209/epl/i2005-10299-3
- [18] A. Corcos, J.-P. Eckmann, A. Malaspinas, Y. Malevergne, D. Sornette, *Imitation and contrarian behaviour: hyperbolic bubbles, crashes and chaos*, *Quantitative Finance* **2** 264 (2002). doi:10.1088/1469-7688/2/4/303
- [19] S. Galam, *Contrarian deterministic effects on opinion dynamics: “the hung elections scenario”*, *Physica A*, **333** 453 (2004). doi:10.1016/j.physa.2003.10.041
- [20] S. Biswas, A. Chatterjee, and P. Sen, *Disorder induced phase transition in kinetic models of opinion dynamics*, *Physica A* **391**, 3257 (2012). doi:10.1016/j.physa.2012.01.046
- [21] S. Galam, *Modeling the Forming of Public Opinion: An approach from Sociophysics*, *Global Economics and Management Review* **18** 2 (2013). doi:10.1016/S2340-1540(13)70002-1
- [22] C. Borghesi and S. Galam, *Chaotic, staggered, and polarized dynamics in opinion forming: The contrarian effect*, *Phys. Rev. E* **73**, 066118 (2006). doi:10.1103/PhysRevE.73.066118
- [23] S. D. Yi, S.K. Baek, C.P. Zhu, B.J. Kim, *Phase transition in a coevolving network of conformist and contrarian voters*, *Phys. Rev. E* **87** 012806 (2013). doi:10.1103/PhysRevE.87.012806
- [24] F. Bagnoli and R. Rechtman, *Topological bifurcations in a model society of reasonable contrarians*, *Phys. Rev. E*, **88** 062914 (2013). doi:10.1103/PhysRevE.88.062914
- [25] F. Bagnoli, R. Rechtman, *Bifurcations in models of a society of reasonable contrarians and conformists*, *Phys. Rev. E* **92**, 042913 (2015). doi:10.1103/PhysRevE.92.042913
- [26] S. E. Asch, *Effects of group pressure on the modification and distortion of judgments*, in *Groups, Leadership and Men*, H. Guetzkow editor, Carnegie Press, Pittsburgh PA (1951), pp. 177–190. S. E. Asch, *Social Psychology*, Prentice Hall, Englewood Cliffs NJ, (1952). S. E. Asch, *Psychological Monographs*, **70d**, 1 (1956).
- [27] S. Biswas, P. Sen, *Model of binary opinion dynamics: Coarsening and effect of disorder*, *Phys. rev. E* **80**, 027101 (2009). doi:10.1103/PhysRevE.80.027101
- [28] S. Biswas, P. Sen, P. Ray, *Opinion dynamics model with domain size dependent dynamics: novel features and new universality class*, *Journal of Physics: Conference Series* **297** (2011) 012003. doi:10.1088/1742-6596/297/1/012003
- [29] D.J. Watts and S.H. Strogatz, *Collective dynamics of ‘small-world’ networks*, *Nature* **393**, 409 (1998). doi:10.1038/30918
- [30] L. Barabási and R. Albert, *Emergence of scaling in random networks*, *Science* **286** 509 (1999). doi:10.1126/science.286.5439.509
- [31] K. Klemm, V. M. Eguiluz, R. Toral and M. San Miguel, *Phys. Rev. E* **67**, 026120 (2003). doi:10.1103/PhysRevE.67.026120
- [32] B. Wu, D. Zhou, and L. Wang, *Evolutionary dynamics on stochastic evolving networks for multiple-strategy games*, *Phys. Rev. E*. **84**, 046111 (2011). doi:10.1103/PhysRevE.84.046111
- [33] P. Holme and M. E. J. Newman, *Nonequilibrium phase transition in the coevolution of networks and opinions*, *Phys. Rev. E* **74**, 056108 (2006). doi:10.1103/PhysRevE.74.056108
- [34] J. Barré, A. Ciani, D. Fanelli, F. Bagnoli, S. Ruffo, *Finite size effects for the Ising model on random graphs with varying dilution*, *Physica A: Statistical Mechanics and its Applications* **388**, 3413 (2009). doi:10.1016/j.physa.2009.04.024
- [35] S. Goswami, S. Biswas, P. Sen, *Complex networks: Effect of subtle changes in nature of randomness*, *Physica A: Statistical Mechanics and its Applications* **390**, 972 (2011). doi:10.1016/j.physa.2010.10.024
- [36] S. Biswas, P. Sen, *Effect of the nature of randomness on quenching dynamics of the Ising model on complex networks*, *Phys. Rev. E* **84**, 066107 (2011). doi:10.1103/PhysRevE.84.066107
- [37] J. Touboul, *The hipster effect: When anti-conformists all look the same*, arXiv:1410.800, <http://arxiv.org/abs/1410.8001v1>
- [38] B. Derrida, *Dynamical Phase Transitions in Spin Models and Automata* in H Beijeren (ed.), *Fundamental Problems in Statistical Mechanics VII*, pp. 276, (Elsevier 1990).
- [39] A.U. Neumann, B. Derrida, *Finite size scaling study of dynamical phase transitions in two dimensional models : Ferromagnet, symmetric and non symmetric spin glasses*, *Journal de Physique* **49**, (1988). doi:10.1051/jphys:0198800490100164700
- [40] E. N. M. Cirillo, F.R. Nardi, A. D. Polosa, *Magnetic order in the Ising model with parallel dynamics*, *Phys. Rev. E* **64**, 057103 (2001). doi:10.1103/PhysRevE.64.057103
- [41] W. B. Arthur, *Inductive Reasoning and Bounded Rationality [The El Farol Problem]*, *The American Economic Review* **84**, 406 (1994).
- [42] D. Challet and Y.-C. Zhang, *Emergence of cooperation and organization in an evolutionary game*, *Physica A*

- 246**, 407 (1997).
- [43] D. Challet and M. Marsili, Y.-C. Zhang, *Minority Games*, Oxford University Press (2005).
- [44] A. C. C. Coolen, *The Mathematical Theory of Minority Games*, Oxford University Press (2005).
- [45] F. Bagnoli, F. Franci, R. Rechtman, *Phase transitions of extended-range probabilistic cellular automata with two absorbing states*, Phys. Rev. E **71**, 046108 (2005). doi:10.1103/PhysRevE.71.046108
- [46] P. S. Dodds, K. D. Harris, and C. M. Danforth, *Limited Imitation Contagion on Random Networks: Chaos, Universality, and Unpredictability*, Phys. Rev. Lett. **110**, 158701 (2013). doi:10.1103/PhysRevLett.110.158701
- [47] K.D. Harris, C.M. Danforth, and P.S. Dodds, *Dynamical influence processes on networks: General theory and applications to social contagion*, Phys. Rev. E **88**, 022816 (2013). doi:10.1103/PhysRevE.88.022816
- [48] L. Boltzmann, *Vorlesungen über Gastheorie*, Leipzig, J. A. Barth, Part I, 1896, Part II, 1898. English translation by S. G. Brush, *Lectures on Gas Theory*, (University of California Press, 1964), Chapter I, Sec. 6.
- [49] M. Suzuki, *Solution and Critical Behavior of Some "Three-Dimensional" Ising Models with a Four-Spin Interaction*, Phys. Rev. Lett. **28**, 507 (1972). doi:10.1103/PhysRevLett.28.507
- [50] C. Castellano, C. Chamon, D. Sherrington, *Quantum mechanical and information theoretic view on classical glass transitions*, Phys. Rev. B **81**, 184303 (2010). doi:10.1103/PhysRevB.81.184303
- [51] F. Bagnoli, T. Matteuzzi, R. Rechtman, *Topological Phase Transitions in the Nonlinear Parallel Ising Model*, Acta Physica Polonica B Proc. Suppl. **9**, 37 (2016). doi:10.5506/APhysPolBSupp.9.37
- [52] F. Bagnoli, T. Matteuzzi, R. Rechtman, *Phase Transitions and Metastable States in the Parallel Ising Model*, Acta Physica Polonica B Proc. Suppl. **9**, 25 (2016). doi:10.5506/APhysPolBSupp.9.25
- [53] E. Ott, *textitChaos in Dynamical Systems* (Cambridge University Press, Cambridge UK, 2002). ISBN: 9780521010849
- [54] A.N. Kolmogorov, *New Metric Invariant of Transitive Dynamical Systems and Endomorphisms of Lebesgue Spaces*, Doklady of Russian Academy of Sciences **119**, N5, 861-864 (1958).
- [55] A.N. Kolmogorov, *Entropy per unit time as a metric invariant of automorphism*, Doklady of Russian Academy of Sciences **124**, 754-755 (1959).
- [56] Ya.G. Sinai, *On the Notion of Entropy of a Dynamical System*, Doklady of Russian Academy of Sciences **124** 768-771 (1959).
- [57] S.H. Strogatz, *Nonlinear Dynamics And Chaos* (Westview Press, Boulder, CO 2015). ISBN: 9780813349107